# NATIONAL ADVISORY COMMITTEE FOR AERONAUTICS

TECHNICAL NOTE 4383

## A COOLED-GAS PYROMETER FOR USE IN HIGH-TEMPERATURE GAS STREAMS

By Lloyd N. Krause, Robert C. Johnson,

and George E. Glawe

Lewis Flight Propulsion Laboratory
Cleveland, Ohio


Washington

September 1958

ADDENDUM

NACA TECHNICAL NOTE 4383

By Lloyd N. Krause, Robert C. Johnson,
and George E. Glawe

September 1958

The logarithmic function on the left hand side of equation (14) (which is also the ordinate for the correlation curve of fig. 8) is applicable to the internal heat-transfer process in which the gas is in equilibrium and the specific heat is essentially constant. However, if the specific heat of the gas changes appreciably during the process of cooling in the probe, it is necessary to treat the process on the basis of enthalpy differences instead of temperature differences. Such is the case, for example, when the measurement is made in a dissociated gas.

If the enthalpy of the gas at station 2 can be determined from knowledge of its composition and temperature, and if the enthalpy of the gas at wall temperature $T_W$ is constant along the tube wall, the terms in the logarithmic function can be replaced by enthalpy terms so that the correlation function becomes

$$\ln\left(\frac{H_0 - H_W}{H_2 - H_W}\right)$$

where

$H_0$ stagnation enthalpy

$H_2$ enthalpy of the gas at temperature $T_2$

$H_W$ enthalpy of the gas at tube wall temperature $T_W$

Thus the instrument is used to determine total stream enthalpy, and the total temperature may then be determined from enthalpy tables.

The relation between enthalpy and temperature for various gases in equilibrium is given in reference 6 and, in addition, references 8, 9, and 10.

8. Huff, Vearl N., Gordon, Sanford, and Morrell, Virginia E.: General Method and Thermodynamic Tables for Computation of Equilibrium Composition and Temperature of Chemical Reactions. NACA Rep. 1037, 1951. (Supersedes NACA TN's 2113 and 2161.)

9. Hall, Eldon W., and Weber, Richard J.: Tables and Charts for Thermodynamic Calculations Involving Air and Fuels Containing Boron, Carbon, Hydrogen, and Oxygen. NACA RM E56B27, 1956.

10. Moeckel, W. E., and Weston, Kenneth C.: Composition and Thermodynamic Properties of Air in Chemical Equilibrium. NACA TN 4265, 1958.



NASA - Langley Field, Va.

NATIONAL ADVISORY COMMITTEE FOR AERONAUTICS

TECHNICAL NOTE 4383

# A COOLED-GAS PYROMETER FOR USE IN HIGH-TEMPERATURE GAS STREAMS

By Lloyd N. Krause, Robert C. Johnson, and George E. Glawe

## SUMMARY

An immersion-type pyrometer is described that utilizes the controlled cooling of a continuously aspirated sample of the gas whose temperature is to be measured. The gas is cooled as it is drawn through a tube, after which its temperature is measured with a thermocouple. Free-stream total temperature is then obtained by a relation involving internal heat transfer in the tube, gas properties, and certain readily measured temperatures and pressures. A technique is described whereby calibration constants obtained in air at near room total temperature are used to compute the high-temperature correlations for other gases with known property values.

Experimental comparison in a high-temperature gas stream with thermocouple probes and with a pneumatic-probe pyrometer showed agreement within 2 percent of total temperature in the range 2000° to 4000° R.

## INTRODUCTION

Thermocouple probes are the most common immersion-type sensing elements used to measure the temperature of high-velocity gases. The selection of the proper thermocouple design for a given application primarily involves compromises between accuracy and structural considerations. As the temperature and velocity of the gas stream are increased, it becomes more difficult to meet the requirements of measurements with thermocouple probes. In fact, many applications exceed the limits of thermocouple designs, even where deliberate use is made of controlled cooling of the thermocouple junction (refs. 1 and 2). Therefore, a definite need exists for other types of immersion pyrometers. Two examples of such types are the pneumatic probe (refs. 3 and 4) and the cooled-tube pyrometer (ref. 2).

The cooled-gas pyrometer reported herein introduces another approach; namely, the controlled cooling of the gas before taking a temperature measurement with a thermocouple. This is accomplished by drawing the

hot gas through a tube with cooled walls. The loss in energy of the gas is reflected by a drop in gas temperature. The amount that the temperature drops is a function of the flow within the tube, gas properties, tube geometry, and tube wall temperature. Therefore, if the temperature of the gas is measured after it has been cooled, and the gas temperature drop can be calculated, then the free-stream gas total temperature can be determined.

This report presents the theory of the cooled-gas pyrometer along with experimental results obtained in both room- and high-temperature gas streams. Room-temperature correlations were made in a total-pressure range from 0.1 to 2.5 atmospheres. High-temperature measurements ranged from 2000° to 4000° R with total pressure from 0.8 to 1.5 atmospheres. All measurements were at subsonic stream Mach numbers. This work is part of the research program in high-temperature measurements being conducted at the NACA Lewis laboratory.



## THEORY

### Convective Heat Transfer in a Tube

Consider an element of length of a tube as shown in the following sketch:

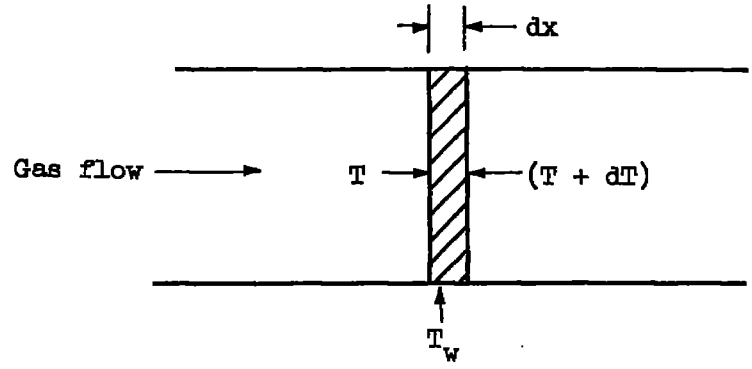


(All symbols are defined in appendix A.)

Since the heat lost by the gas is equal to the heat transferred to the wall,

$$h(T_b - T_w)dx = -\frac{D}{4} Gc_p dT_b \qquad (1)$$

If $(T_b - T_w)$ is represented by the expression $K(T - T_w)$, where $K$ and $T_w$ are assumed constant, then $dT_b = K\,dT$, and equation (1) can be stated as follows:

$$\frac{4}{D}\,dx = -\frac{dT}{St(T - T_w)} \tag{2}$$

It will be assumed that, over a limited Reynolds number range, the Stanton number can be expressed as follows:

$$St = \frac{C}{Re_f^a Pr^b}\, f\left(Re_f, \frac{x}{D}\right) \tag{3}$$

The viscosity in $Re_f$ is based on film temperature $T_f$, which is defined as $(T + T_w)/2$. The Prandtl number is assumed to be constant over the film-temperature range within the tube. Since both the cross-sectional area of the tube and the mass-flow rate within the tube are constant, the Reynolds number within the tube varies only because of the viscosity. The Reynolds number $Re_f$ within the tube can be expressed as

$$Re_f = \frac{Re_c}{(\mu_f/\mu_c)} \tag{4}$$

where the subscript c refers to the location of the thermocouple. The factor $f\left(Re_f, \frac{x}{D}\right)$ in equation (3) is introduced to account for deviations in the Stanton number because of undeveloped flow near the tube entrance and the effect of tube curvature.

It will be assumed that

$$f\left(Re_f, \frac{x}{D}\right) \approx f\left(Re_c, \frac{x}{D}\right) \tag{5}$$

and if equations (3), (4), and (5) are substituted in equation (2), the result is

$$\frac{C}{Re_c^a Pr^b}\, f\left(Re_c, \frac{x}{D}\right) \frac{dx}{D} = \frac{-dT}{\left(\frac{\mu_f}{\mu_c}\right)^a (T - T_w)} \tag{6}$$

Since

$$T = T_0 \qquad \text{at} \qquad x = 0$$

$$T = T_c \qquad \text{at} \qquad x = l$$

and assuming

$$\int_0^l f\left(\mathrm{Re}_c, \frac{x}{D}\right)\frac{dx}{D} \approx C\mathrm{Re}_c^{\epsilon}$$

the integral form of equation (6) becomes

$$\frac{C}{\mathrm{Re}_c^{a_1}\mathrm{Pr}^b} = \int_{T_c}^{T_0} \frac{dT}{\left(\frac{\mu_f}{\mu_c}\right)^a (T - T_w)} \approx \int_{T_c}^{T_0} \frac{dT}{\left(\frac{\mu_f}{\mu_c}\right)^{a_1} (T - T_w)} \tag{7}$$

with $a_1 = a - \epsilon$ where $|\epsilon|$ is much smaller than $|a|$. Since the Prandtl number varies only slightly for most gases, it is difficult to establish the power of the Prandtl number in equation (7) by any calibration technique. Reference 5 in a similar situation suggests a value of 2/3 for b. This value of b will be assumed for this investigation.

In equation (7) it will be assumed that over the range of temperatures involved, the viscosity $\mu$ can be expressed as

$$\left(\frac{\mu}{\mu_r}\right)^{a_1} = \alpha T + C \tag{8}$$

where $\mu_r$ is an arbitrary reference viscosity that is chosen as the viscosity of air at 1000° R. Figure 1 gives the value of $\alpha$ for various gases for a range of values of $a_1$ over a temperature range from 800° to 2300° R. The maximum absolute error in the value of $(\mu/\mu_r)^{a_1}$ between that tabulated in reference 6 and that calculated by the preceding equation is 3 percent.

The use of this relation to evaluate $(\mu_f/\mu_c)^{a_1}$ in equation (7) yields

$$\frac{C}{\mathrm{Re}_c^{a_1}\mathrm{Pr}^{2/3}} = \int_{T_c}^{T_0} \frac{dT}{\left[1 + \frac{\alpha}{(\mu_c/\mu_r)^{a_1}} (T_f - T_c)\right](T - T_w)} \tag{9}$$

The solution of equation (9) is

$$\ln\left(\frac{T_0 - T_w}{T_c - T_w}\right) = \frac{C}{Re_c^{a_1} Pr^{2/3}} + \ln(1 + \xi) \approx \frac{C}{Re_c^{a_1} Pr^{2/3}} + \xi \qquad (10)$$

where the approximation assumes $|\xi|$ much less than 1, and

$$\xi = \frac{\frac{1}{2}\alpha\beta(e^{\psi} - 1) - \left(1 - \frac{1}{2}\alpha\beta\right)(e^{\psi\alpha\beta} - 1)}{e^{\psi\alpha\beta}\left(1 - \frac{1}{2}\alpha\beta\right) - \frac{1}{2}\alpha\beta e^{\psi}}$$

$$\beta = \frac{T_c - T_w}{(\mu_c/\mu_r)^{a_1}}$$

$$\psi = \frac{C}{Re_c^{a_1} Pr^{2/3}}$$

4855

## Application of Theory to Probe Design

The term $\xi$ in equation (10) accounts for the effects of the variation in gas viscosity along the tube for the case $T_0 \gg T_w$. This term can be controlled to some extent by probe design, because its magnitude is influenced by geometry. It can also be seen that, for the case where $T_0$ approaches $T_w$, the viscosity variation is negligible and $\xi$ becomes zero. In any case $\xi$ may be treated as a correction factor, and the general correlation parameters are related by

$$\ln\left(\frac{T_0 - T_w}{T_c - T_w}\right) \approx \frac{C}{Re_c^{a_1} Pr^{2/3}} \qquad (11)$$

Figure 2 is a schematic diagram of a cooled-gas pyrometer. The gas is drawn into the probe at station 1 and is cooled while passing through the inside tube whose wall temperature is essentially constant. At station 2 the gas has been cooled sufficiently to obtain a measurement of temperature ($T_2$) with a thermocouple located in the center of the tube. A tapered body is attached to the thermocouple shaft and acts as a flow nozzle whose minimum area is the flow passage between the body and the tube wall at station 3. The pressure downstream of this section (measured by pressure tap $p_4$) must be sufficiently low to maintain critical flow through the nozzle.

The correlation equation shows that it is necessary to evaluate Reynolds number $Re_c$ in the tube and gas temperature $T_c$ at a measuring station $x = l$. Station 2 (fig. 2) represents this measuring station in the probe. The Reynolds number can be expressed as

$$Re_2 = \frac{4\dot{m}}{\pi D_2 \mu_2} \tag{12}$$

where $D_2$ is the inside diameter of the inner tube, $\mu_2$ is the viscosity of gas at $T_2$, and $\dot{m}$ is the mass-flow rate of the gas in the tube.

The mass-flow rate $\dot{m}$ is determined by the following relation for critical flow through a nozzle:

$$\dot{m} = \frac{C_d A_3 P_2}{\sqrt{T_2}} \left[ \gamma \left( \frac{M}{R} \right) \left( \frac{2}{\gamma + 1} \right)^{\frac{\gamma+1}{\gamma-1}} \right]^{1/2} \tag{13}$$

where $\gamma$ and $M$ are evaluated at temperature $T_2$, and $A_3$ is the minimum flow area of the nozzle.

For the sake of simplifying the Reynolds number correlation, it can be assumed that the total-pressure drop in the tube is small ($P_2 \approx P_0$), and evaluation of $C_d$ is not necessary since $C_d$ is in turn a function of Reynolds number. With those simplifying assumptions, and combining equations (11), (12), and (13), the "working" equation of the probe becomes

$$\ln \left( \frac{T_0 - T_w}{T_2 - T_w} \right) \approx \left( C \times Pr^{-2/3} \right) \left[ f(M,\gamma) \right]^{-a_1} \left( \frac{P_0}{\frac{\mu_2}{\mu_r} \sqrt{\frac{T_2}{1000}}} \right)^{-a_1} \tag{14}$$

where

$$f(M,\gamma) = \left[ \sqrt{M\gamma} \left( \frac{2}{\gamma + 1} \right)^{\frac{\gamma+1}{2\gamma-2}} \right]$$

(see nomogram, fig. 3) with $\mu_r$ the arbitrary reference viscosity, taken as viscosity of air at 1000° R, and with Pr, $\mu_2$, M, and $\gamma$ evaluated at $T_2$.

For a given probe design, the constant and the quantity $a_1$ may be evaluated by calibrating the probe with air at near room temperature if

a sufficient difference exists between $T_2$ and $T_w$. The measured quantities would be $T_0$, $T_w$, $T_2$, and $P_0$.

Thus, if $\log\left[\ln\left(\frac{T_0 - T_w}{T_2 - T_w}\right)\right]$ is plotted against $\log\left\{\left[f(M,\gamma)\right]\left(\frac{P_0}{\frac{\mu_2}{\mu_r}\sqrt{\frac{T_2}{1000}}}\right)\right\}$, the slope of the curve will determine the value of $a_1$ and the intercept will be the term $(C \times Pr^{-2/3})$. The constant is then calculated with knowledge of the value of Pr at temperature $T_2$. After $a_1$ and the constant are determined for a given probe, the probe can then be used for high-temperature measurements of other gases if the gas property values are known.

Strictly speaking, equation (14) cannot be applied to high-temperature operation ($T_0 \gg T_w$) with the same degree of rigor as it applies to the ambient calibration ($T_0 \approx T_w$). One of the differences existing between the two cases has been previously discussed - namely, the variation of viscosity along the tube when ($T_0 \gg T_w$); this variation is accounted for by the $\xi$ term in equation (10).

The correction term $\xi$ is defined in equation (10) and includes a factor $\alpha$ which is defined in equation (8) and evaluated for certain gases in figure 1. For a probe application,

$$\beta \approx \frac{T_2 - T_w}{\left(\frac{\mu_2}{\mu_r}\right)^{a_1}}$$

$$\psi \approx \ln\left(\frac{T_0 - T_w}{T_2 - T_w}\right)$$

The correction term $\xi$ is presented as a function of $\alpha$, $\beta$, and $\psi$ in figure 4.

Other factors that have not been explicitly included in equation (14) and that will introduce deviations for the case ($T_0 \gg T_w$) are:

(1) Critical-flow area of the nozzle $A_3$ will decrease as the tapered insert is heated.

(2) The $T_2$ term on the right side of equation (14) will deviate from gas bulk temperature because of a temperature profile.

(3) The indicated temperature $T_2$ will be low because of a radiation error.

(4) The viscosity $\mu_2$ will not be equal to $\mu_c$ because of the error in $T_2$.

However, for the probe design herein reported and for the range of tests, these factors were of small magnitude or of a cancelling nature, so that equation (14) represented a good approximation. Furthermore, these deviations are often insignificant compared to the uncertainties in the knowledge of gas properties for high-temperature application.

Appendix B presents an analysis of these deviations and includes terms that can be applied to equation (14) to correct for them, and a sample calculation is presented in appendix C.

## APPARATUS

A detailed drawing of the cooled-gas pyrometer is shown in figure 5. The pyrometer consists of three concentric tubes, the largest tube having an outside diameter of 1/2 inch. The hot gas passes through the 1/4-inch tube; cooling water passes through the two annuli. Inlet water is passed next to the 1/4-inch tube to minimize the effect of external heat received by the outside tube. Spacing rods, shown in section A-A, are located in the annuli to ensure uniform cross sections in the region of the bend. The inlet nozzle is machined from Inconel and heliarc-welded in place. The thermocouple insert head centers the junction as well as serving as a flow nozzle. The critical-flow section is a square inscribed in a circle, chosen because of the ease in controlling dimensions. A pressure tap located downstream of the thermocouple monitors the pressure at the downstream side of the critical-flow section and also acts as a total-pressure tap when the aspiration is shut off. Three probes were built and tested to determine the reproducibility of this design.

High-temperature evaluation tests were performed in the high-temperature water-cooled tunnel described in reference 2. Two types of thermocouple probes and one pneumatic temperature probe were used as comparison instruments. One probe type was a bare-wire, crossflow, platinum-rhodium - platinum thermocouple with a water-cooled support. Radiation, conduction, and recovery corrections were applied to this configuration by using methods and values from references listed in the bibliography of reference 2. The other thermocouple probe was a sonic-aspirated platinum-rhodium - platinum type as described in reference 7.

The pneumatic probe was primarily of importance in obtaining total temperature in the range beyond that of the thermocouples. It was used exclusively in the range from 3600° to 4000° R. This probe utilized the design and operation criteria and methods of computation presented in reference 4.

In operating ranges where all three comparison probes could be used to obtain total temperature, agreement to within 1.5 percent of the mean temperature of the three instruments was obtained.

To determine the constants in the working equation (eq. (14)), room-temperature tests were performed in a $2\frac{3}{4}$-inch-diameter variable-density tunnel. Because of the relatively small differences between total, indicated, and water-coolant temperatures in the room-temperature tests, differential temperature measurements instead of absolute measurements were made. The temperature-difference terms $(T_0 - T_w)$ and $(T_2 - T_w)$ appearing in the temperature correlation were thus obtained directly.

## PROCEDURE AND RESULTS

### Preliminary Tests

In the process of developing the cooled-gas pyrometer, several preliminary tests were performed to verify assumptions and to find the effects of varying design and operational factors. These tests and the results obtained are discussed in this section.

Axial location of thermocouple. - Considerations of the relation between $T_2$ and gas properties indicated that it is desirable that $T_2$ be large, so that the uncertainty in knowledge of property values becomes less important. However, at large values of $T_2$, radiation errors associated with the thermocouple must be considered. Therefore, a compromise must be made in selecting the distance from the inlet to station 2. For the range of conditions and probe design (fig. 5) herein reported, a fixed location of 80 tube diameters from the inlet was chosen as a compromise. The axial temperature profile along the centerline of the tube was measured by moving the thermocouple insert. Figure 6(a) shows the result of a typical test of this type and indicates the sensitivity to axial positioning.

Radial location of thermocouple. - At an axial position of 80 diameters from the inlet, the thermocouple junction was displaced radially from the centerline. The resultant radial temperature profile in the tube is shown in figure 6(b).

Choice of temperature measurement to represent $T_w$ in correlation parameter. - As presented in theory, $T_w$ is the temperature of the inner wall of the center 1/4-inch-diameter tube. Assuming that the temperature drop across the wall of the tube is negligible, it is reasonable that $T_w$ can be represented by measurement of coolant temperature. A series of tests was therefore performed in the high-temperature range, and measurements were made of cooling-water inlet and outlet temperature and of temperature rise in the inner and outer cooling annuli. These tests indicated that the coolant temperature rise in the inner passage was small and could be neglected for correlation purposes; thus, coolant-inlet temperature $T_W$ could be used to represent $T_w$.

In one of the above-mentioned tests the normal coolant-flow rate was decreased as much as possible without damaging the probe. The coolant inlet temperature was fixed, and the coolant temperature rise through the probe increased by a factor of three. During this time the thermocouple insert measurement $T_2$ remained constant, thus establishing the fact that, even under the most marginal coolant flows, $T_W$ would represent $T_w$ as a correlation parameter.

Effect of aspiration rate. - As previously indicated, this probe depends on aspiration for its operation and includes a critical-flow section at station 3 (fig. 2). This design feature was incorporated for convenience in determining the mass-flow rate and the Reynolds number in the inner tube. It also conveniently controls the flow in the tube so that the correlation is independent of free-stream Mach number. This is advantageous because in many applications only approximate values of flow conditions are known.

The results of a test to establish the effect of aspiration rate on the thermocouple insert indication are presented in figure 6(c). A pressure ratio of approximately 0.5 is required to maintain critical flow at the nozzle portion of the thermocouple insert. It is seen from the figure that at least this critical pressure ratio should be maintained across the probe to ensure a constant probe indication.

An interesting result is that with the aspiration shut off, the thermocouple $T_2$ will indicate $T_W$. This leads to a simple mode of operation when using the probe in a hot gas; that is, with the aspiration off, the thermocouple insert will yield cooling-water temperature $T_W$ and the $p_4$ tap will measure total pressure $P_0$. Then, with aspiration on, a measurement of $T_2$ will complete the measurements required to obtain total temperature. No independent measurements of cooling-water temperature or total pressure are required if time is available to operate the probe in this manner. These remarks apply to both subsonic and supersonic streams, where for the supersonic case $P_0$ would be the total pressure behind the normal shock formed by the probe.

Pressure drop in tube. - To verify the assumption of negligible pressure drop within the 1/4-inch tube, tests were performed at both ambient- and high-temperature conditions with a total-pressure tube replacing the thermocouple insert. With the sensing end of the total-pressure tube located at the normal axial position of the thermocouple junction, a constant total-pressure loss of 4 percent of stream total pressure was obtained. Because of the fact that the percentage pressure drop was constant, a correlation Reynolds number evaluated at station 2 (fig. 2) was based on $P_0$ instead of $P_2$. This simplified the probe design and operation in that it was not necessary to have an internal total-pressure measurement at station 2.

Cooling-water flow rate. - Figure 7 presents variation of water-flow rate with variation of water pressure drop across the probe. About 1.6 gallons per minute are passed with a pressure drop of 50 pounds per square inch.

## Final Tests

Using the results obtained from the preliminary tests, a cooled-gas pyrometer was tested at both ambient and high temperatures with the thermocouple junction located 80 tube diameters downstream of the probe entrance. Room-temperature measurements were made in a total-pressure range from 0.1 to 2.5 atmospheres. High-temperature measurements ranged from 2000° to 4000° R with the total pressure ranging from 0.8 to 1.5 atmospheres. Free-stream Mach numbers for all measurements were subsonic and ranged from 0.1 to 1.0.

The correlation for the final probe configuration is shown in figure 8, with the abscissa plotted both in terms of Reynolds number and in terms of parameters in working equation (14) that are proportional to Reynolds number.

Both room- and high-temperature tests are included in figure 8, with 35 percent of the 118 data points in the 2000° to 4000° R range. For convenience, two straight lines, computed by the method of least squares, have been drawn through the data, with equal weight assigned to both room- and high-temperature points. The data fall within a band of ±2 percent in $(T_0 - T_w)$, the probable error of a single observation being ±1 percent. The slope of the main portion of the curve is -0.348; above a Reynolds number of 27,000 the slope is -0.160. The range of Reynolds numbers covered in testing the cooled-gas pyrometer is not complete enough to establish the slope at lower Reynolds numbers, but it is reasonable to assume that the slope will change when flow inside the tube is completely laminar. Therefore, the extrapolation of figure 8 to lower Reynolds numbers is questionable because of the uncertainty of the transition to laminar flow.

Two other pyrometers, made from the same drawing as that of figure 5, were also tested. The results are presented as the dashed lines of figure 8. Although the correlation curves of the three probes are similar in shape and in their probable errors, the slopes are slightly different and the curves are displaced by amounts up to 15 percent of $(T_O - T_W)$. Geometry factors that may produce these differences are as follows:

(1) Differences in tube diameter

(2) Variation in tube diameter and cross-sectional shape

(3) Differences in size and shape of nozzle portion of thermocouple insert

(4) Varying surface roughness inside tube

From these considerations it would be difficult if not impractical to control the fabrication to the point where reproducible results would be obtained between probes. Therefore, it is advisable to obtain the correlation curve by individual calibration.

## CONCLUDING REMARKS

A pyrometer whose principle of operation is based on measurements of the controlled cooling of a continuously aspirated sample of gas has been described and evaluated. Such an instrument is of use in making local temperature measurements above the usual range attributed to thermocouples.

Probe correlation curves obtained from both room-temperature and high-temperature evaluations showed agreement within ±2 percent, which was the same as the order of accuracy of the high-temperature comparison instruments used to establish stream total temperature.

The operation of the probe is relatively simple, and the correlation is independent of free-stream Mach number. However, the accuracy depends directly on the knowledge of gas properties, and the probe must initially be calibrated. In applications where the gas properties are not known accurately enough to establish acceptable absolute measurements, the instruments may still be used for temperature profile measurements.

Lewis Flight Propulsion Laboratory
National Advisory Committee for Aeronautics
Cleveland, Ohio, August 8, 1958

## APPENDIX A

## SYMBOLS

| | |
|---|---|
| $A$ | cross-sectional flow area |
| $C$ | a constant |
| $C_d$ | discharge coefficient |
| $c_p$ | specific heat at constant pressure |
| $D$ | inside diameter of aspirated tube |
| $G$ | mass-flow rate per unit area |
| $h$ | convective heat-transfer coefficient |
| $l$ | axial distance from tube inlet to measuring station |
| $M$ | molecular weight |
| $\dot{m}$ | mass-flow rate |
| $P$ | total pressure |
| $Pr$ | Prandtl number |
| $p$ | static pressure |
| $R$ | universal gas constant |
| $Re$ | Reynolds number |
| $Re_c$ | internal Reynolds number with viscosity evaluated at $T_c$ |
| $Re_f$ | internal Reynolds number with viscosity evaluated at $T_f$ |
| $St$ | Stanton number |
| $T$ | total gas temperature in center of tube at any axial position $x$ |
| $T_b$ | gas bulk temperature in tube |
| $T_c$ | gas temperature in center of tube at measuring station $x = l$ |
| $T_f$ | gas film temperature, $\frac{T + T_w}{2}$ |

$T_W$ temperature of inlet cooling water

$T_w$ temperature of inside tube wall

$T_0$ total gas temperature of free stream

$T_2$ gas temperature in center of tube as indicated by thermocouple inserted at measuring station 2

x axial distance from tube entrance

$\gamma$ ratio of specific heats

$\mu$ viscosity

$\mu_c$ viscosity evaluated at $T_c$

$\mu_f$ viscosity evaluated at $T_f$

$\mu_r$ reference viscosity (air at $1000^\circ$ R)

$\mu_2$ viscosity evaluated at $T_2$

Probe station notation:

0 free stream

1 tube entrance

2 internal measuring station

3 critical-flow section

4 pressure-tap position

## APPENDIX B

## FACTORS CONTRIBUTING TO DEVIATIONS NOT EXPLICIT IN WORKING EQUATION

A more rigorous statement of equation (14) would be

$$\ln\left(\frac{T_0 - T_w}{T_c - T_w}\right) = C\left(\frac{A_{3C}}{A_{3H}}\right)^{a_1} Pr^{-2/3}\left[f(M,\gamma)\right]^{-a_1}\left(\frac{P_0}{\frac{\mu_c}{\mu_r}\sqrt{\frac{T_b}{1000}}}\right)^{-a_1} + \xi \qquad (B1)$$

### Radiation Effect

The indicated thermocouple temperature $T_2$ will not be equal to $T_c$ when $T_2 > T_w$ because of a radiation loss from the thermocouple junction to the cold walls. A radiation correction factor $\epsilon_R$ can be defined such that

$$T_c = T_2(1 + \epsilon_R) \qquad (B2)$$

### Viscosity Effect

The viscosity $\mu_c$ at the measuring station should be evaluated at the corrected temperature $T_c$ instead of at $T_2$. The viscosity correction factor $\epsilon_\mu$ will be defined so that

$$\mu_c = \mu_2(1 + \epsilon_\mu) \qquad (B3)$$

### Temperature-Profile Effect

The temperature $T_c$ will not represent bulk temperature $T_b$ when a temperature profile exists in the tube; therefore, a relation for these two terms must be established. Thus, $\epsilon_b$ will be defined so that

$$T_b = T_c(1 - \epsilon_b) \qquad (B4)$$

### Nozzle-Area Effect

When the tapered body that forms the critical-flow area is heated, the critical-flow area hot $A_{3H}$ will be less than the critical-flow

area cold $A_{3C}$; the relation between areas and this correction factor $\epsilon_n$ can be defined so that

$$\frac{A_{3C}}{A_{3H}} = 1 + \epsilon_n \tag{B5}$$

## Total Correction

If the preceding corrections are substituted in equation (B1), and the magnitudes of $\epsilon_R$, $\epsilon_\mu$, $\epsilon_b$, and $\epsilon_n$ are assumed to be much less than 1, the result is

$$\ln\left(\frac{T_0 - T_w}{T_2 - T_w}\right) = C \times Pr^{-2/3}\left[f(M,\gamma)\right]^{-a_1}\left(\frac{P_0}{\frac{\mu_2}{\mu_r}\sqrt{\frac{T_2}{1000}}}\right)^{-a_1} \times$$

$$\left\{1 + a_1\left[\epsilon_\mu + \epsilon_n - \frac{1}{2}\left(\epsilon_b - \epsilon_R\right)\right]\right\} + \epsilon_R\left(\frac{T_2}{T_2 - T_w}\right) + \xi \tag{B6}$$

## Evaluation of Correction Factors

Radiation. - The radiation correction for a spike-type thermocouple is approximately one-third greater than that for a bare-wire crossflow probe:

$$\epsilon_R \approx 0.036\ \epsilon_{CA}\sqrt{\frac{d}{N_M p}}\left(\frac{T_2}{1000}\right)^{2.82}\left[1 - \left(\frac{T_w}{T_2}\right)^4\right] \tag{B7}$$

where the gas is air.

For the probe design herein reported, the Mach number $N_M$ in the tube is about 0.2, the wire diameter d is 0.020 inch, and the average emittance $\epsilon_{CA}$ of the Chromel-Alumel wire can be taken as 0.75. Introducing these values into equation (B7),

$$\epsilon_R \approx \frac{0.0087}{\sqrt{P_0}}\left(\frac{T_2}{1000}\right)^{2.82}\left[1 - \left(\frac{T_w}{T_2}\right)^4\right] \tag{B8}$$

where $P_0$ is in atmospheres.

Bulk temperature. - For fully developed turbulent flow, reference 8 implies the following expression for the relation between bulk temperature $T_b$ and the temperature in the center of the tube $T_c$:

$$T_b \approx T_c \left(1 - 0.18 \frac{T_c - T_w}{T_c}\right) \tag{B9}$$

Substituting this equation into equation (B4) and solving for $\epsilon_b$ give

$$\epsilon_b = 0.18 \frac{T_c - T_w}{T_c} \approx 0.18 \frac{T_2 - T_w}{T_2} \tag{B10}$$

Nozzle expansion. - The relation for the critical-flow area $A_{3H}$ when the tapered plug is at elevated temperature $T_2$ and the area $A_{3C}$ when the plug is at the cold-wall temperature $T_w$ is given by

$$A_{3H} = A_{3C} \left[1 - 2\delta \left(\frac{A_2}{A_{3C}} - 1\right)(T_2 - T_w)\right] \tag{B11}$$

where $\delta$ is the coefficient of linear expansion of the plug material.

Substituting equation (B11) into equation (B5) yields

$$\epsilon_n = 2\delta \left(\frac{A_2}{A_{3C}} - 1\right)(T_2 - T_w) \tag{B12}$$

Viscosity. - Since the viscosities of most gases are functions of the gas temperature to approximately the 0.7 power, $\epsilon_\mu$ may be expressed as

$$\epsilon_\mu \approx 0.7\ \epsilon_R \tag{B13}$$

## APPENDIX C

## SAMPLE CALCULATIONS

As an example, assume that a temperature measurement is to be made in a flow system using high-temperature air. The correlation curve for the probe to be used will be represented by the lower curve of figure 8. This curve can be identified by two straight lines, over the range of Reynolds numbers shown, so that

| | Range I | Range II |
|---|---|---|
| $Re_2$ | 6,000-27,000 | 27,000-60,000 |
| $a_1$ | 0.348 | 0.160 |
| Intercept | 1.57 | 1.045 |
| Constant | 1.24 | 0.825 |

where the value of the constant (eq. (14)) is found from

$$C = \text{Intercept} \times Pr^{2/3}$$

with the correlation gas Prandtl number being 0.7.

The primary measurements taken with the probe will be assumed to be as follows:

$$P_0 = 1.5 \text{ atm}$$

$$T_W = 520^\circ \text{ R}$$

$$T_2 = 1620^\circ \text{ R}$$

The property values of the gas at temperature $T_2$ are

$$\gamma = 1.34$$

$$Pr = 0.70$$

$$M = 29$$

$$\mu_2 = 0.815 \times 10^{-6} \text{ lb-sec/sq ft}$$

The following correlation parameters are then evaluated:

$f(M,\gamma)$ from nomogram (fig. 3) . . . . . 3.6
$\mu_2/\mu_r$ . . . . . 1.36

where $\mu_r$ is a reference viscosity (air at 1000° R). Therefore,

$$f(M,\gamma)\left(\frac{P_0}{\frac{\mu_2}{\mu_r}\sqrt{\frac{T_2}{1000}}}\right) = 3.6\left(\frac{1.5}{1.36\sqrt{1.62}}\right)$$

$$= 3.13$$

This quantity is the value of the abscissa for the curve (fig. 8) which corresponds to that range of the curve where

$$a_1 = 0.348$$

$$C = 1.24$$

The slope is equal to $a_1$, and the constant $C$ is the probe constant in the working equation (14) so that

$$\ln\left(\frac{T_0 - T_w}{T_2 - T_w}\right) \approx C \times Pr^{-2/3} \times \left[f(M,\gamma)\right]^{-a_1}\left[\frac{P_0}{\left(\frac{\mu_2}{\mu_r}\right)\sqrt{\frac{T_2}{1000}}}\right]^{-a_1}$$

$$\approx (1.24)(0.7)^{-2/3}(3.6)^{-0.348}\left(\frac{1.5}{1.36\sqrt{1.62}}\right)^{-0.348}$$

$$\approx 1.055$$

Therefore,

$$\left(\frac{T_0 - T_w}{T_2 - T_w}\right) \approx 2.87$$

$$T_0 \approx 2.87(1620 - 520) + 520$$

$$\approx 3680° \text{ R}$$

A more rigorous relation for calculating $T_0$ appears in appendix B, in which several factors are added to equation (14) and appear as correction factors in equation (B6).

Evaluation of these terms as applied to the sample case is as follows: From equation (B8),

$$\epsilon_R \approx \frac{0.0087}{\sqrt{1.5}} (1.62)^{2.82} \left[1 - \left(\frac{520}{1620}\right)^4\right]$$

$$\approx 0.0277$$

From (B10),

$$\epsilon_b \approx 0.18\left(\frac{1620 - 520}{1620}\right)$$

$$\approx 0.122$$

From (B12),

$$\epsilon_n = 2(7.0\times10^{-6})(2.75 - 1)(1620 - 520)$$

$$= 0.027$$

From (B13),

$$\epsilon_\mu \approx 0.7\ \epsilon_R$$

$$\approx (0.7)(0.0277)$$

$$\approx 0.0194$$

From figure 1,

$$\alpha = 1.69\times10^{-4}$$

By definition,

$$\beta \approx \frac{T_2 - T_w}{\left(\frac{\mu_2}{\mu_r}\right)^{a_1}}$$

$$\approx \frac{1620 - 520}{(1.36)^{0.348}}$$

$$\approx \frac{1100}{1.113}$$

Therefore,

$$\alpha\beta \approx 0.167$$

and

$$\psi \approx \ln\left(\frac{T_0 - T_w}{T_2 - T_w}\right)$$

$$\approx 1.055$$

4855

previously evaluated from the general working equation (14). Therefore, from figure 4,

$$\xi = -0.024$$

Substituting the calculated values in equation (B6) yields

$$\ln\left(\frac{T_0 - T_w}{T_2 - T_w}\right) = 1.055\{1.00\} + 0.041 - 0.024$$

$$= 1.072$$

Therefore,

$$\frac{T_0 - T_w}{T_2 - T_w} = 2.92$$

$$T_0 = 2.92(1620 - 520) + 520$$

$$= 3730^\circ \text{ R}$$

Therefore, for the given sample computation the difference between a solution using equation (14) and one using equation (B6) would be 1.3 percent. This difference of 1.3 percent, however, should not be taken to imply a small magnitude in the total correction for all cases. In general, the significant terms in the correction factors will be the last two terms in equation (B6).

## REFERENCES

1. Matton, G., and Fouré, C.: Thermoelectric Probes for Measuring High Temperatures in Gas Streams: Their application to the Study of Flames Stabilized by Obstacles. Sixth Symposium (International) on Combustion, Reinhold Pub. Corp., 1956, pp. 757-763.

2. Warshawsky, I.: Pyrometry of High Velocity Gases. Sixth Symposium (International) on Combustion, Reinhold Pub. Corp., 1956, pp. 739-750.

3. Baker, Dwight I.: Mixture Ratios and Temperature Surveys of Ammonia-Oxygen Rocket Motor Combustion Chambers. Jet Prop., vol. 25, no. 5, May 1955, pp. 217-226.

4. Simmons, Frederick S., and Glawe, George E.: Theory and Design of a Pneumatic Temperature Probe and Experimental Results Obtained in a High-Temperature Gas Stream. NACA TN 3893, 1957.

5. McAdams, William H.: Heat Transmission. Third ed., McGraw-Hill Book Co., Inc., 1954, eqs. 9-10b, p. 219.

6. Hilsenrath, Joseph, et al.: Tables of Thermal Properties of Gases. Cir. 564, NBS, Nov. 1, 1955.

7. Glawe, George E.: A High Temperature Combination Sonic Aspirated Thermocouple and Total Pressure Probe. Jet Prop., vol. 27, no. 5, May 1957, pp. 543-544.

8. Eckert, E. R. G.: Introduction to the Transfer of Heat and Mass. McGraw-Hill Book Co., Inc., 1950.

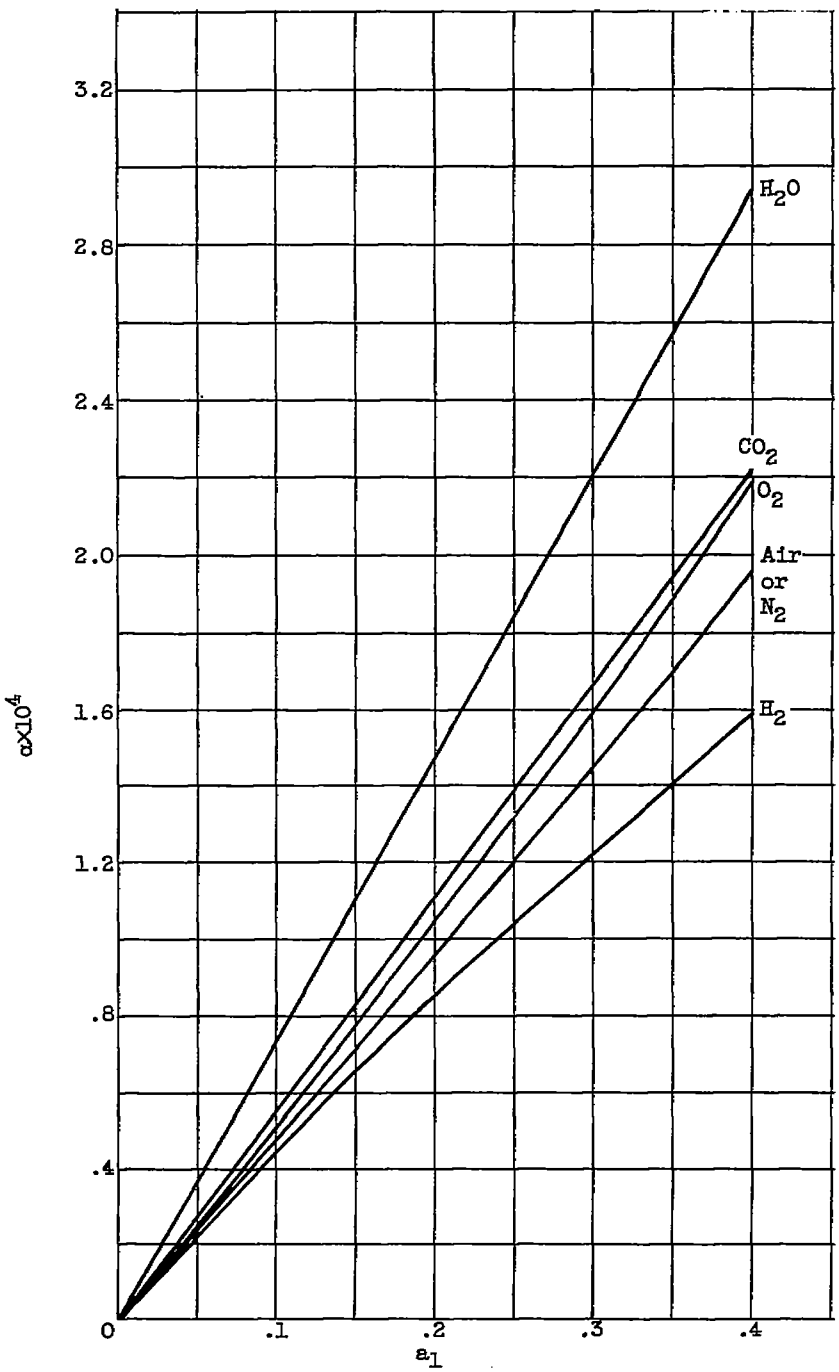


Figure 1. - Variation of $\alpha$ with $a_1$ for several gases.

$$\alpha = \frac{\Delta\left(\frac{\mu}{\mu_r}\right)^{a_1}}{\Delta T}.$$

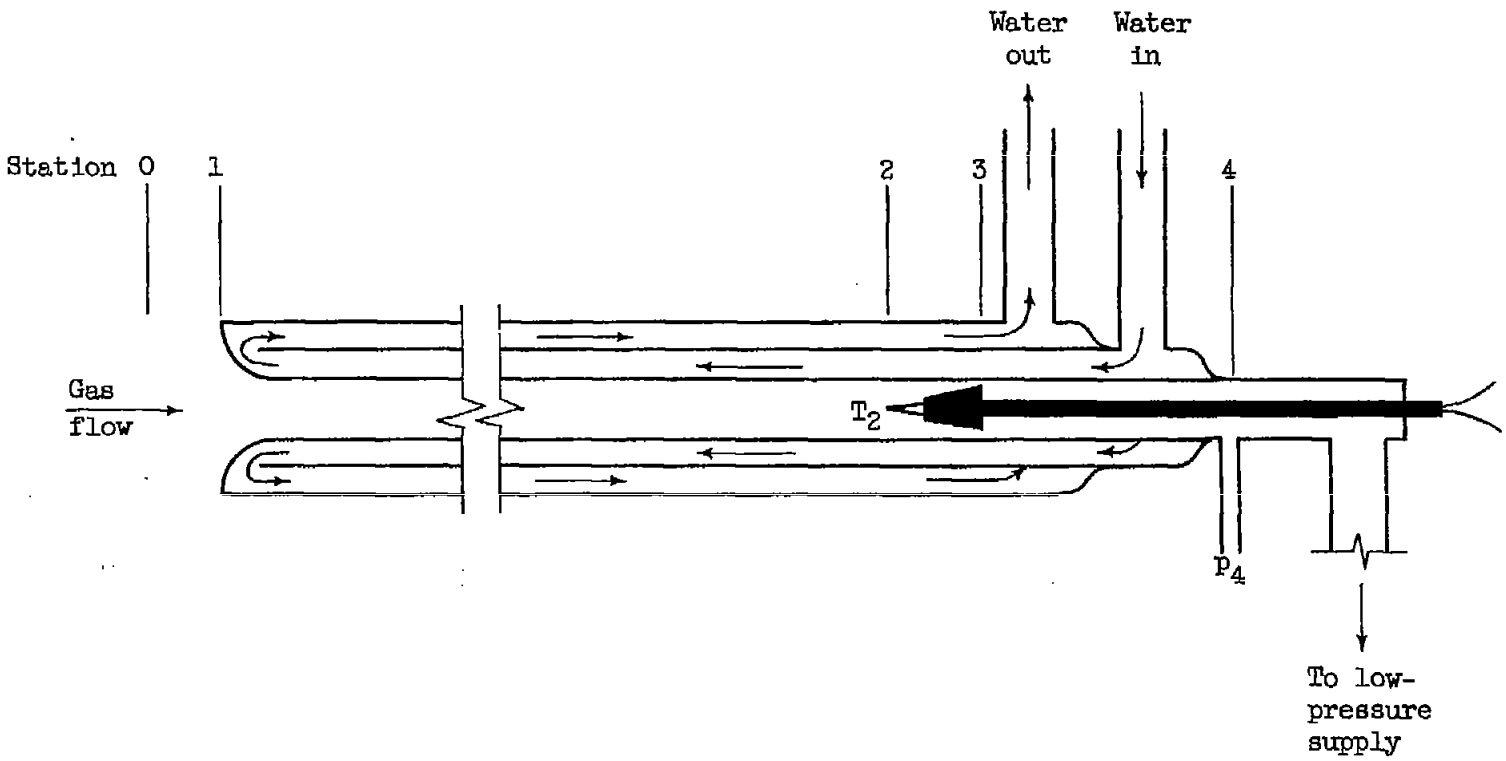


Figure 2. - Schematic diagram of cooled-gas pyrometer.

$$f(M,\gamma) = \left[\sqrt{M\gamma}\left(\frac{2}{\gamma+1}\right)^{\frac{\gamma+1}{2\gamma-2}}\right]$$

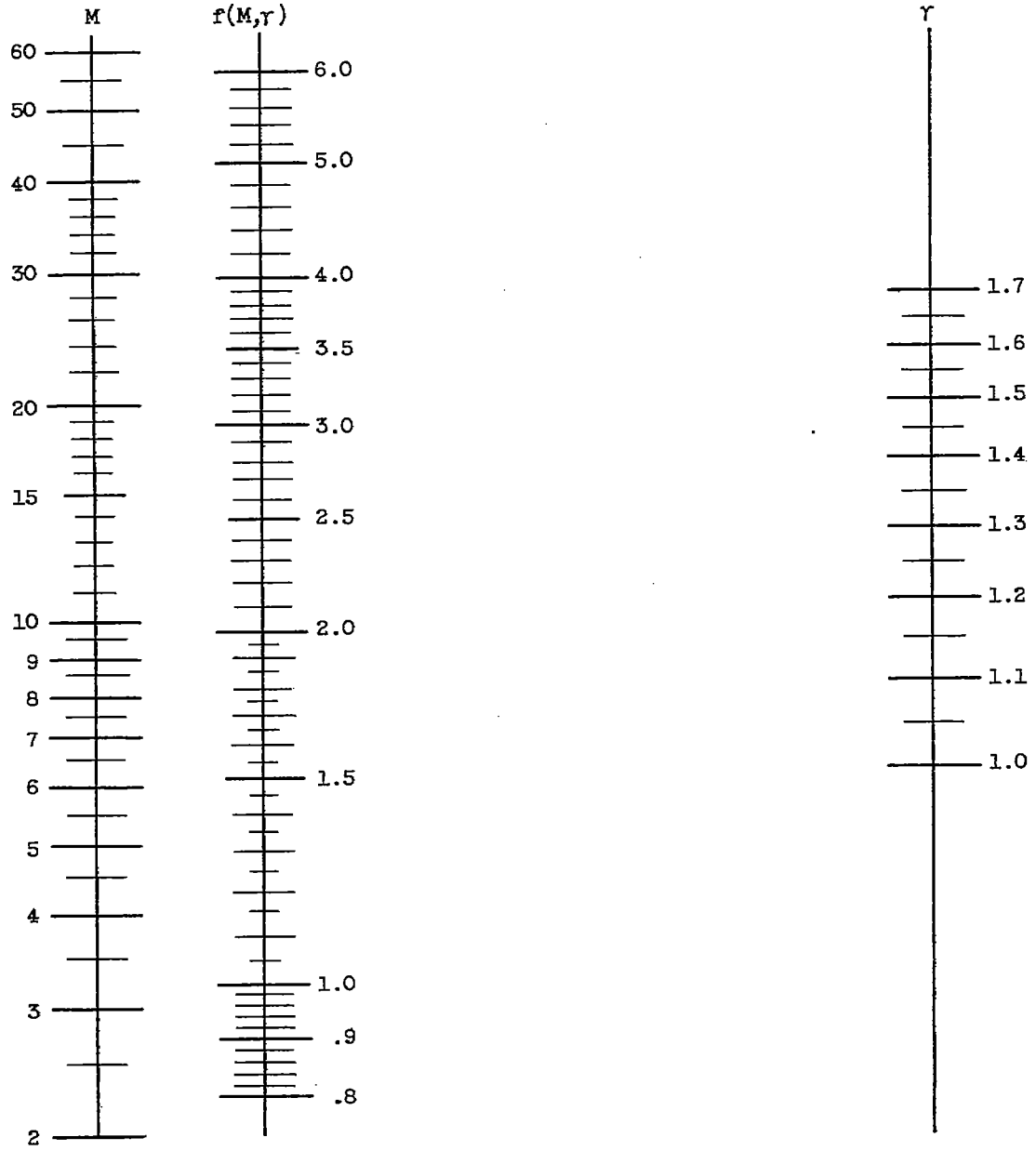


Figure 3. - Nomogram for function of molecular weight and ratio of specific heats.

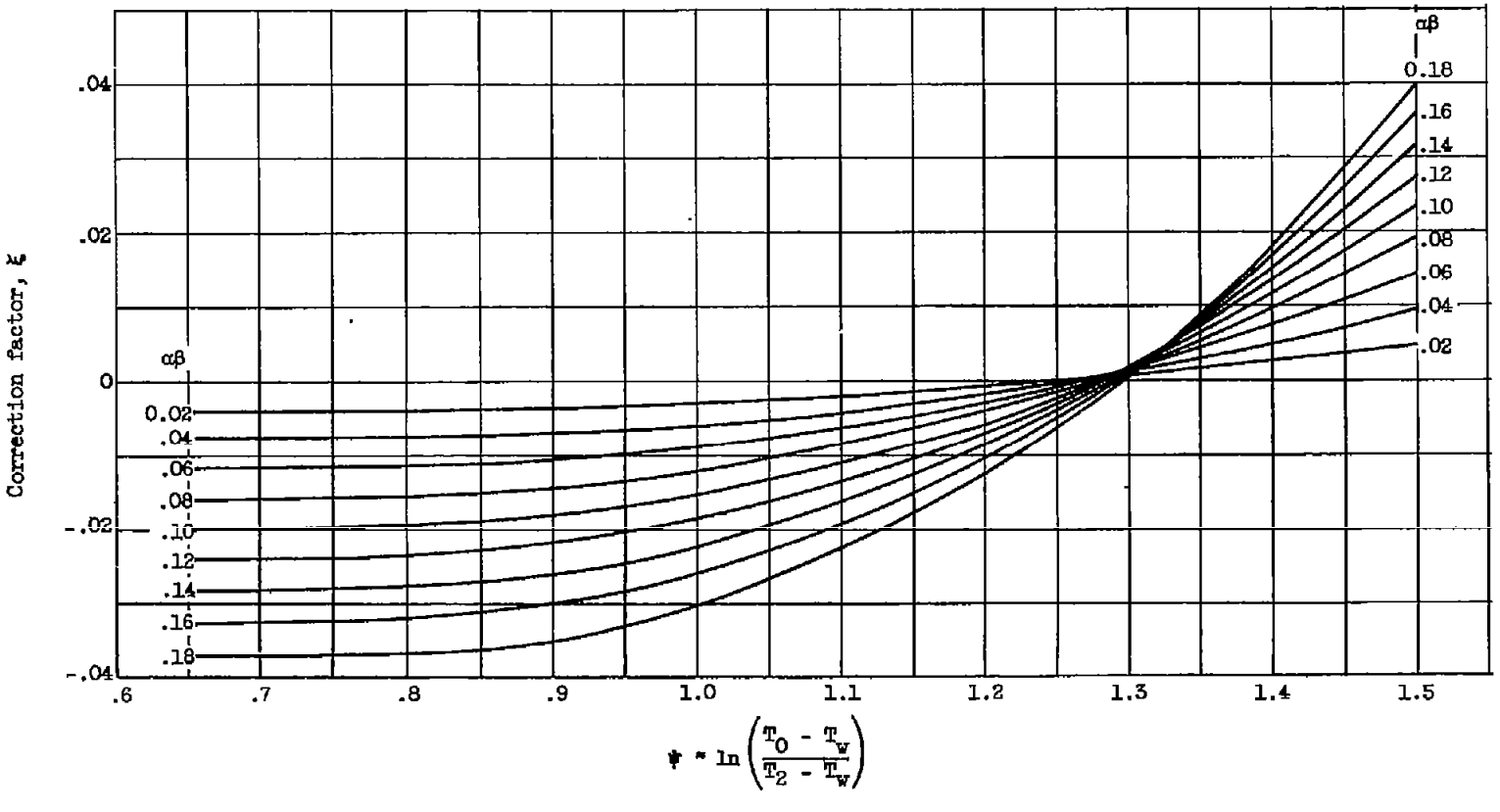


Figure 4. - Variation of correction factor $\xi$ with correlation parameters.

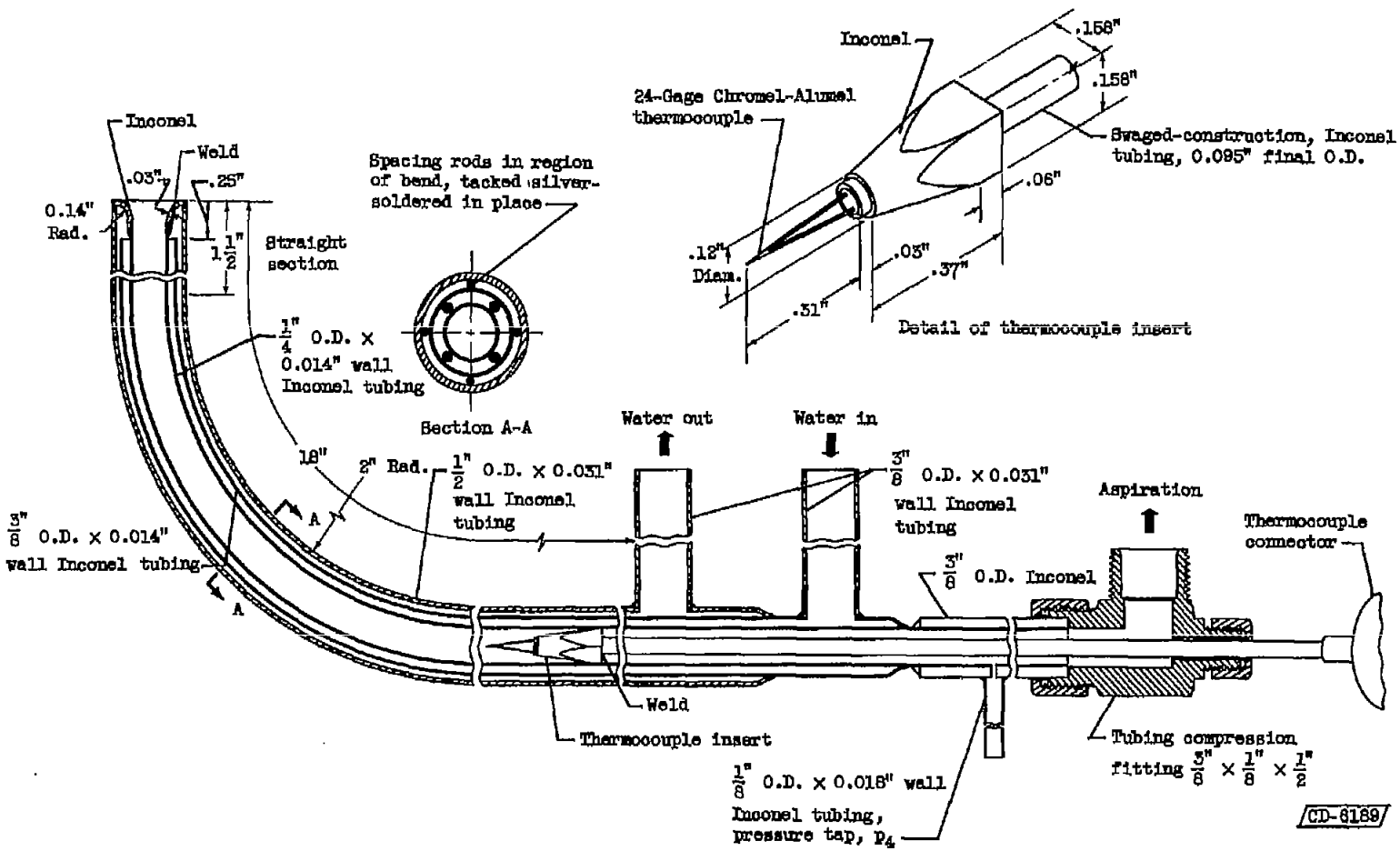


Figure 5. - Probe details.

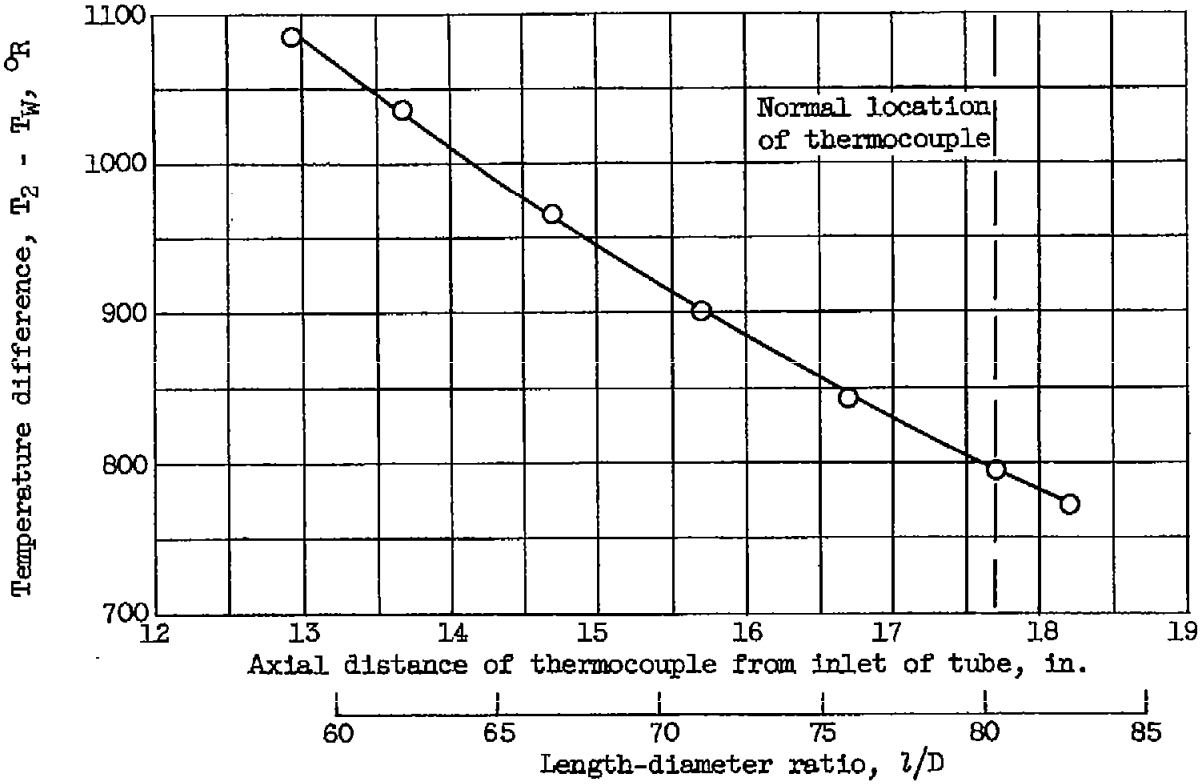


(a) Variation of axial location of thermocouple. Total temperature, 2730° R; total pressure, 1.16 atmospheres.

Figure 6. - Variation of probe indication with change in axial or radial location of thermocouple or aspiration rate. Water temperature, 500° R.

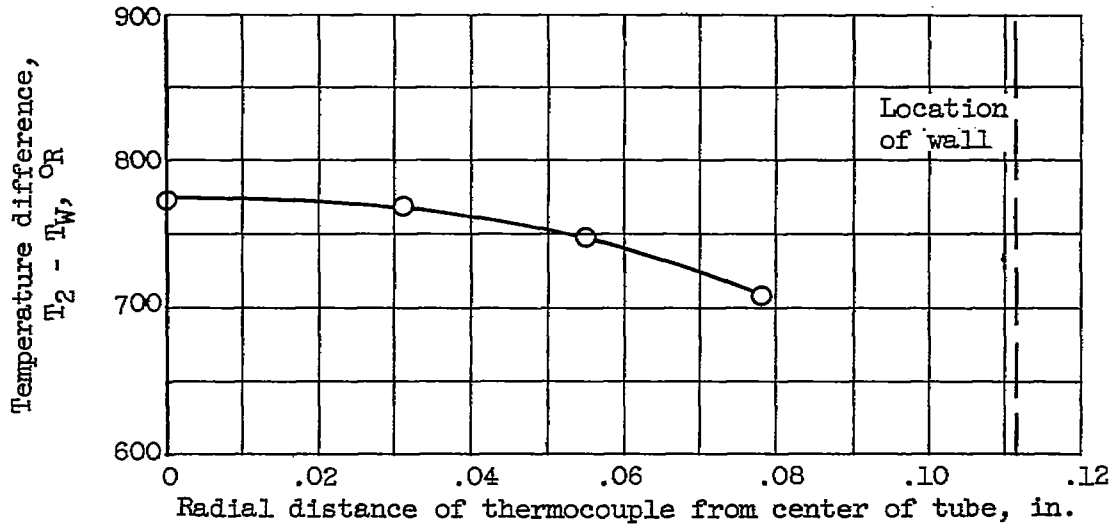


(b) Variation of radial location of thermocouple. Total temperature, 2850° R; total pressure, 0.94 atmosphere.

Figure 6. - Continued. Variation of probe indication with change in axial or radial location of thermocouple or aspiration rate. Water temperature, 500° R.

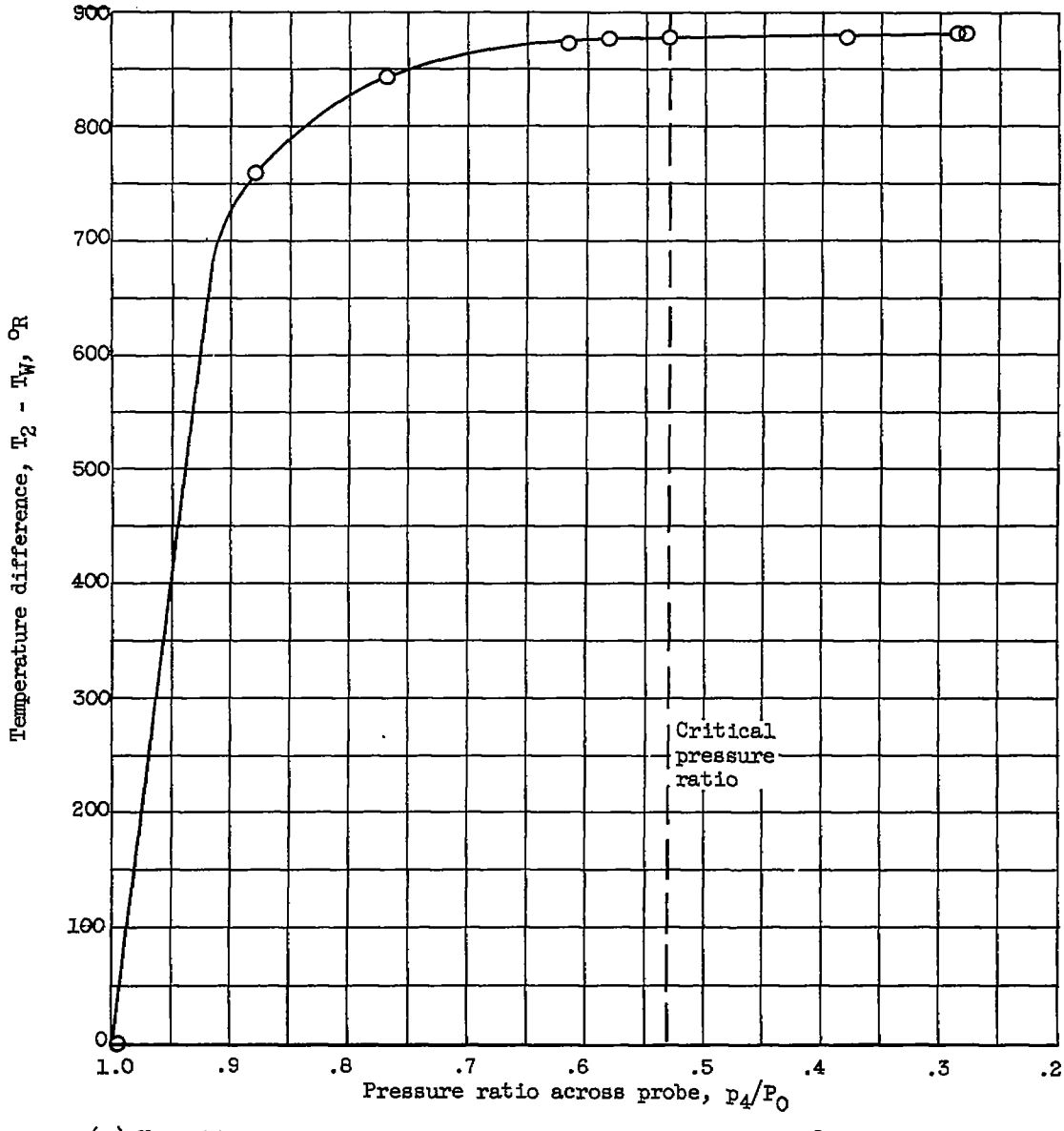


(c) Variation of aspiration rate. Total temperature, 3070° R; total pressure, 1.11 atmospheres.

Figure 6. - Concluded. Variation of probe indication with change in axial or radial location of thermocouple or aspiration rate. Water temperature, 500° R.

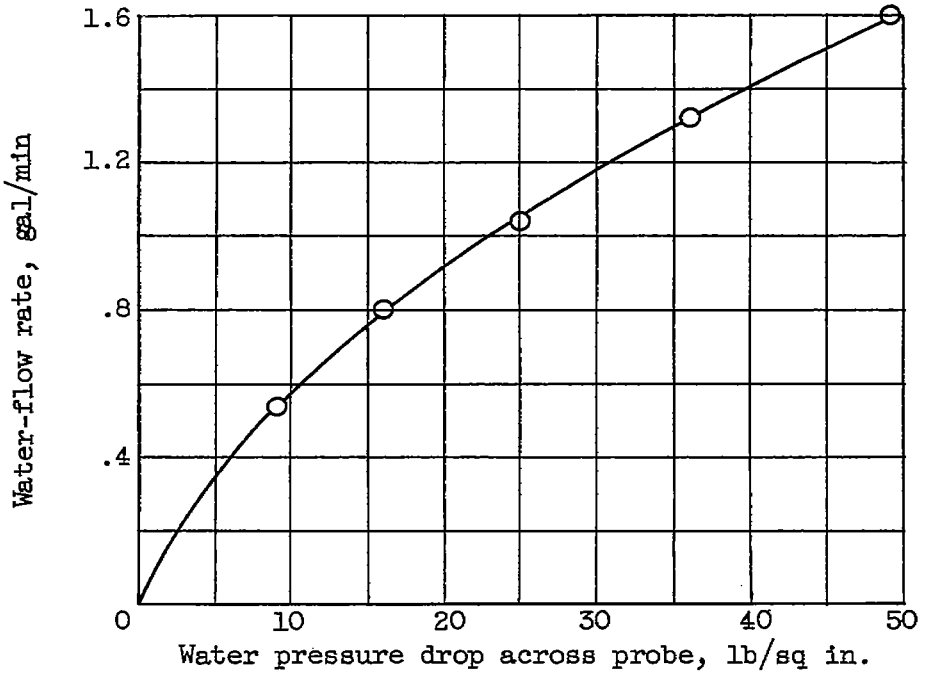


Figure 7. - Variation of water-flow rate with water pressure drop across probe.

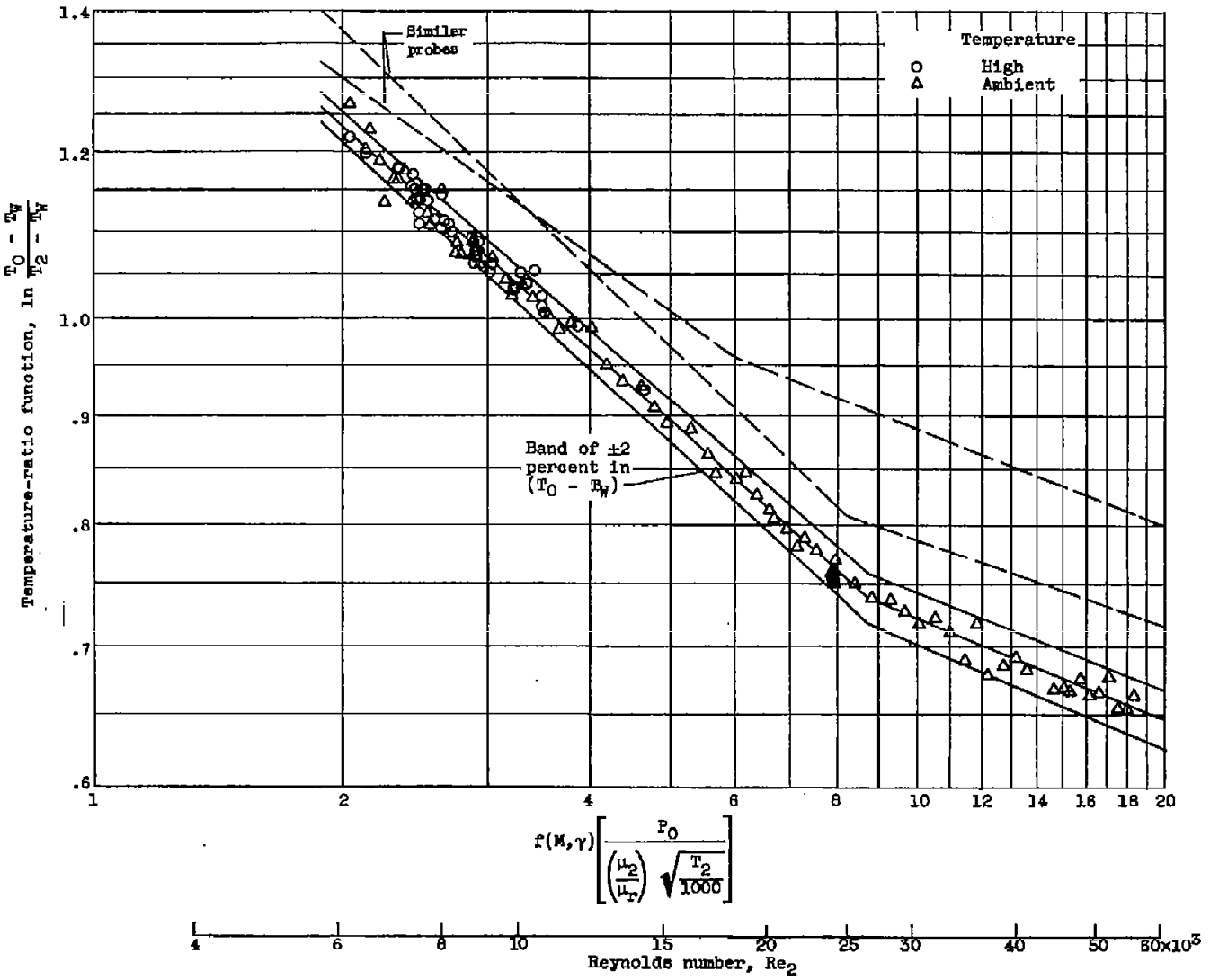


Figure 8. - Correlation curve.





NACA - Langley Field, Va.